SUPPORTING INFORMATION

Enhanced Thermal Transportation of Flexible Composite Films Across Electrostatic Self-assembly of Black Phosphorene and Boron Nitride Nanosheets

Yandong Wang[a,b], Xianzhe Wei[b], Huiwu Cai[a], Bin Zhang[a], Yapeng Chen[b], Maohua Li[b], Yue Qin[b], Linhong Li[b,c], Xiangdong Kong[b], Ping Gong[b,c], Huanyi Chen[b], Xinxin Ruan[b], Chengcheng Jiao[b], Tao Cai[b], Wenying Zhou[*,a], Zhongwei Wang[*,d], Kazuhito Nishimura[e], Cheng-Te Lin[b,c], Nan Jiang[b,c], Jinhong Yu[*,b,c]

[a]*School of Chemistry and Chemical Engineering, Xi'an University of Science & Technology, Xi'an 710054, China*

[b]*Key Laboratory of Marine Materials and Related Technologies, Zhejiang Key Laboratory of Marine Materials and Protective Technologies, Ningbo Institute of Materials Technology and Engineering, Chinese Academy of Sciences, Ningbo 315201, China.*

[c]*Center of Materials Science and Optoelectronics Engineering, University of Chinese Academy of Sciences, Beijing 100049, China.*

[d]*Shandong University of Science and Technology, College of Materials Science and Engineering, Qingdao 266590, China.*

[e]*Advanced Nano-processing Engineering Lab, Mechanical Engineering, Kogakuin University, Tokyo, 192-0015, Japan.*

Correspondence and requests for materials should be addressed to W. Zhou (E-mail: wyzhou2004@163.com), W. Wang (Email: wangzhongwei@fusilinchem.com) or J. Yu (Email: yujinhong@nimte.ac.cn)

Supplementary Materials

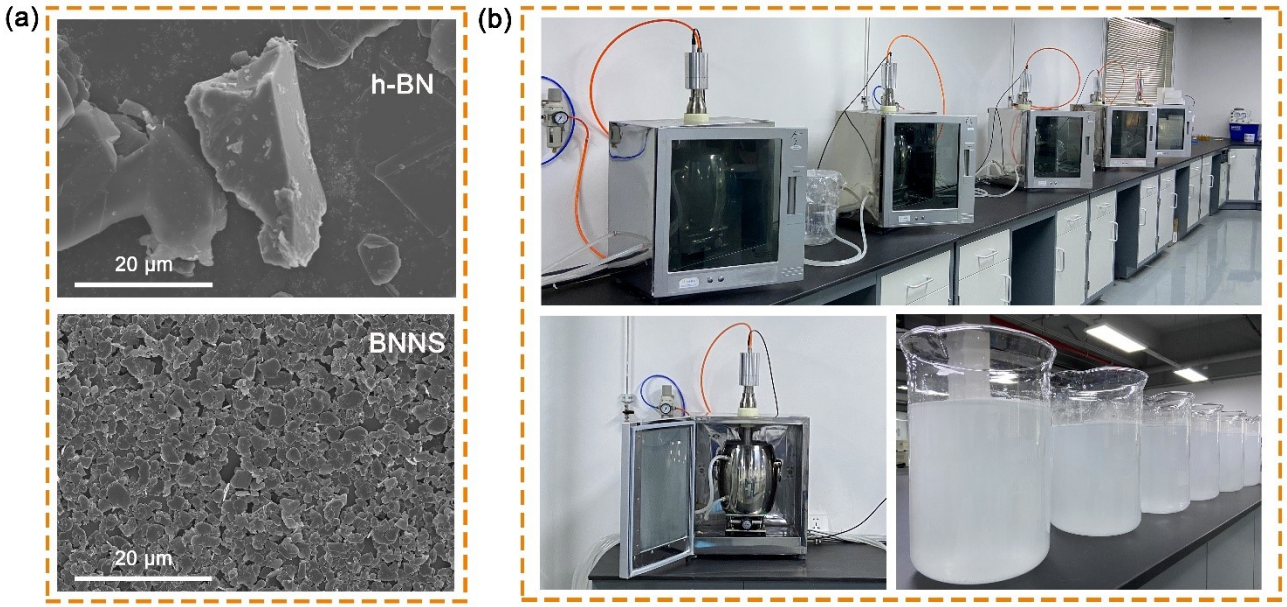

Figure S1. (a) SEM image of h-BN and BNNS; (b) The optical image of the whole home-made cutting-edge ultrasonic equipment (above) and the collected BNNS dispersion (right).

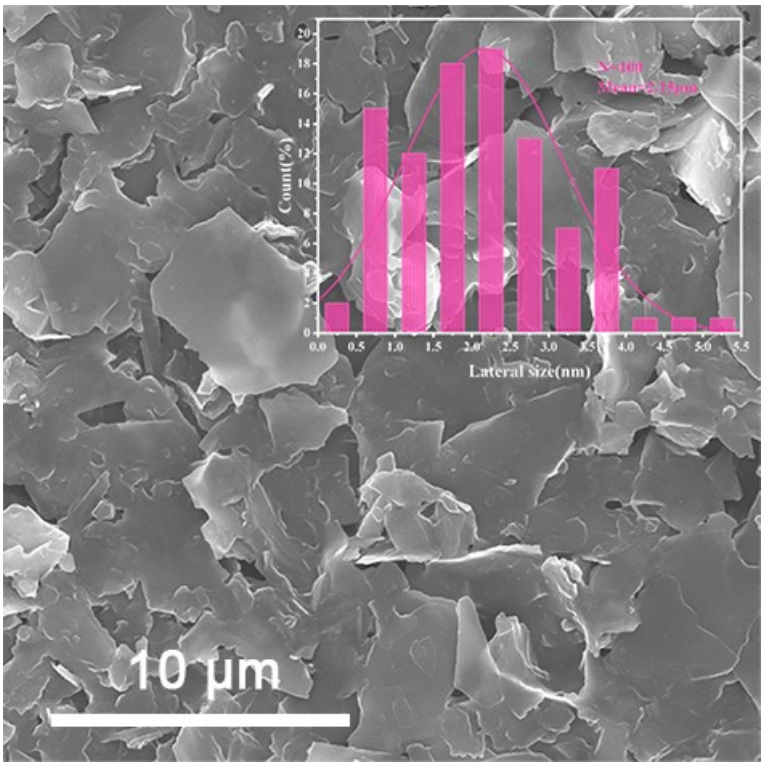

Figure S2. SEM image of black phosphorene nanosheets (inset is the particle size distribution curve)

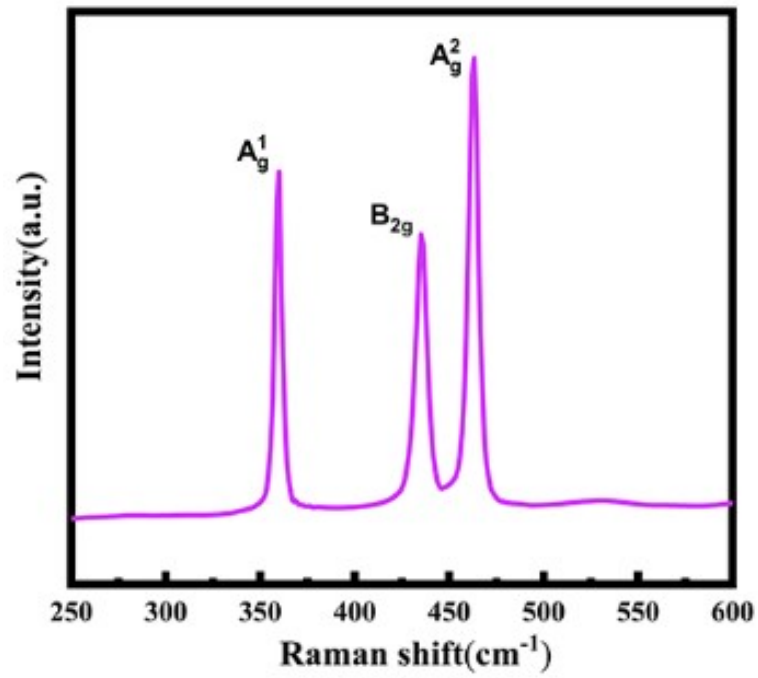

Figure S3. Raman pattern of the BP

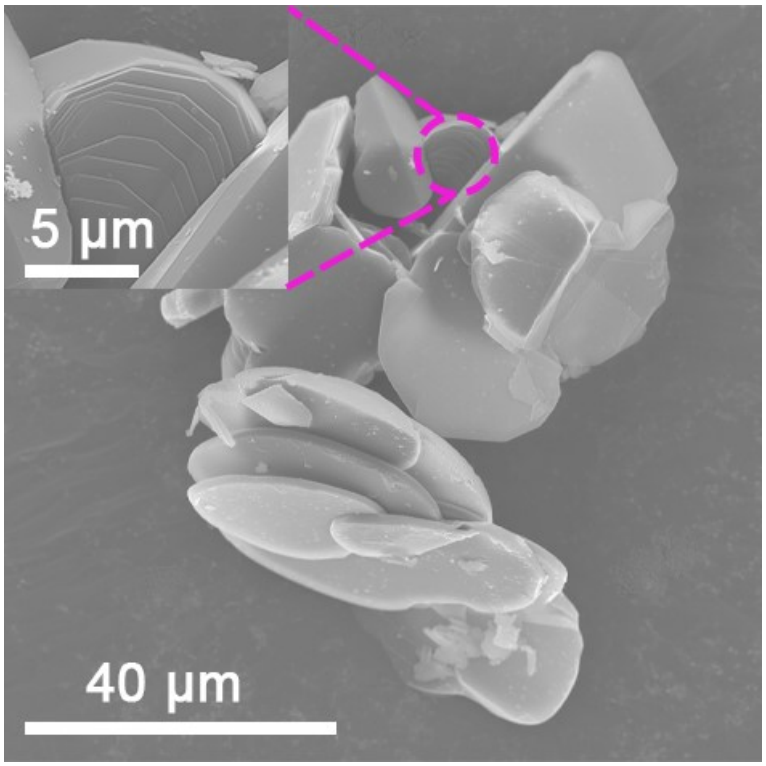

Figure S4. SEM image of pristine h-BN

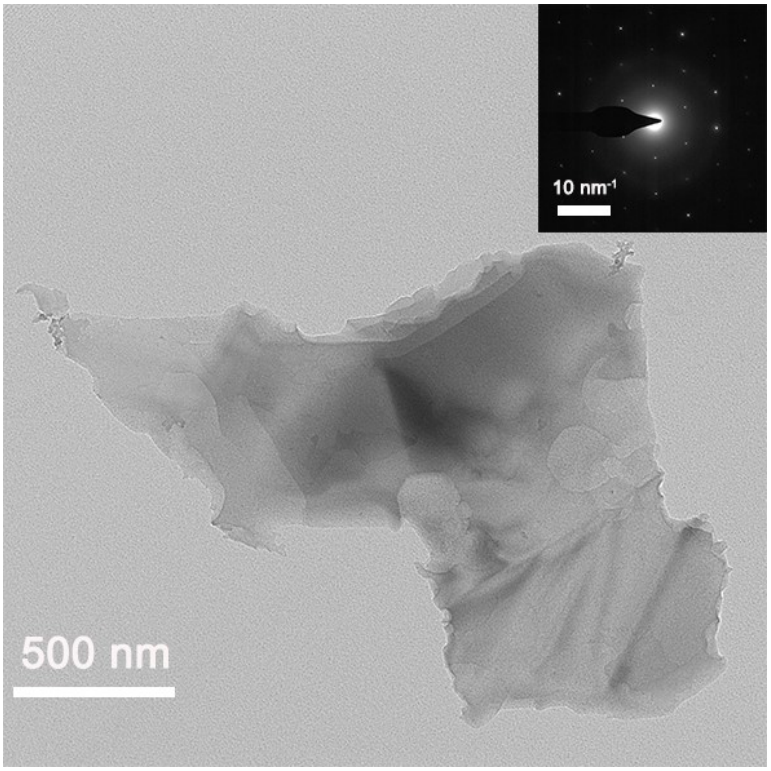

Figure S5. TEM image of BNNS

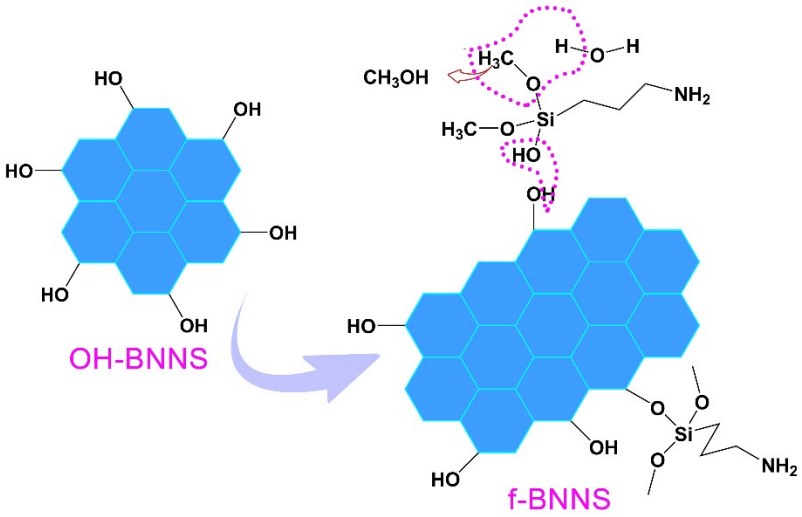

Figure S6. Surface modification process of BNNS

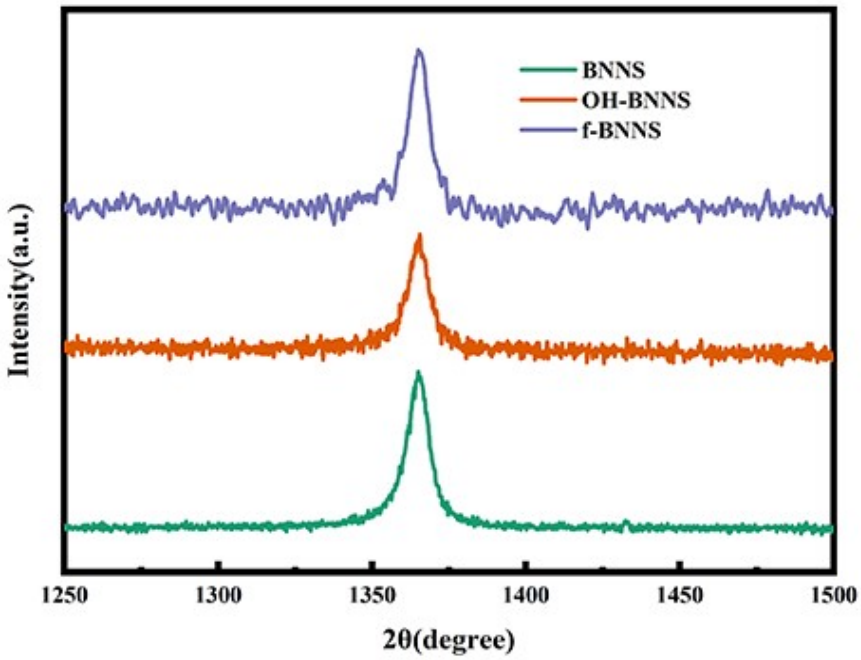

Figure S7. Raman spectra of BNNS, OH-BNNS, and functionalized BNNS (*f*-BNNS).

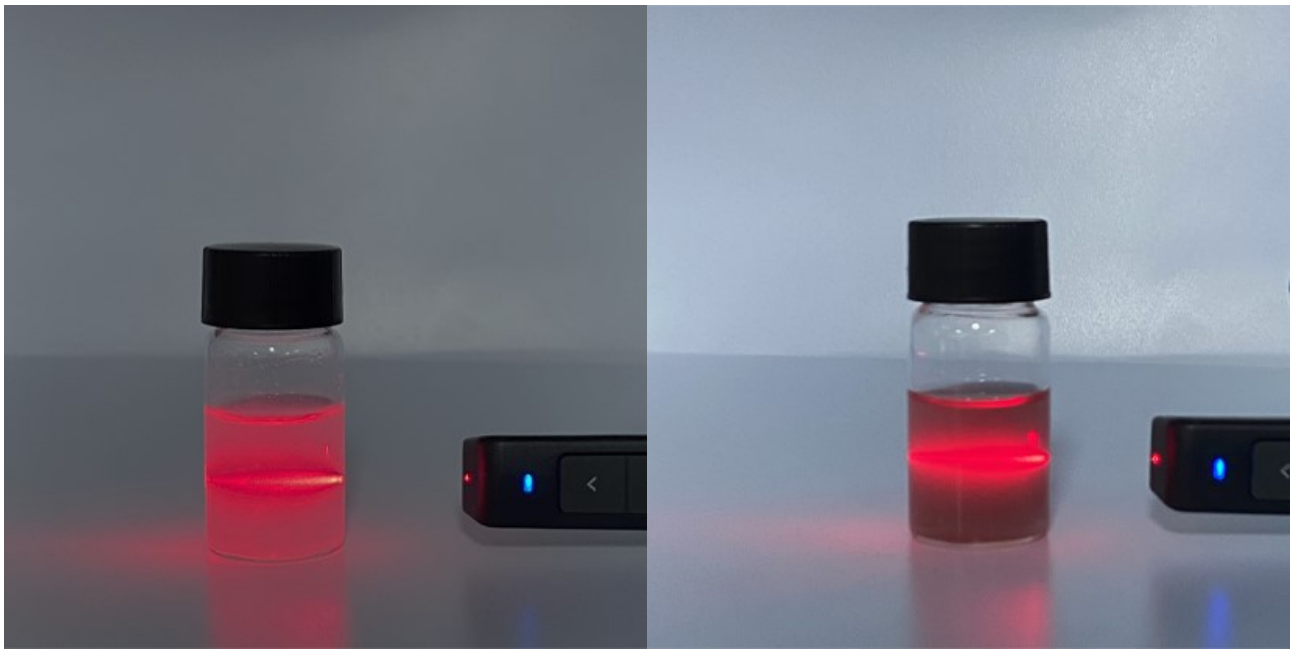

Figure S8. Optical image of BP and *f*-BNNS suspension showing the "Dyndall effect".

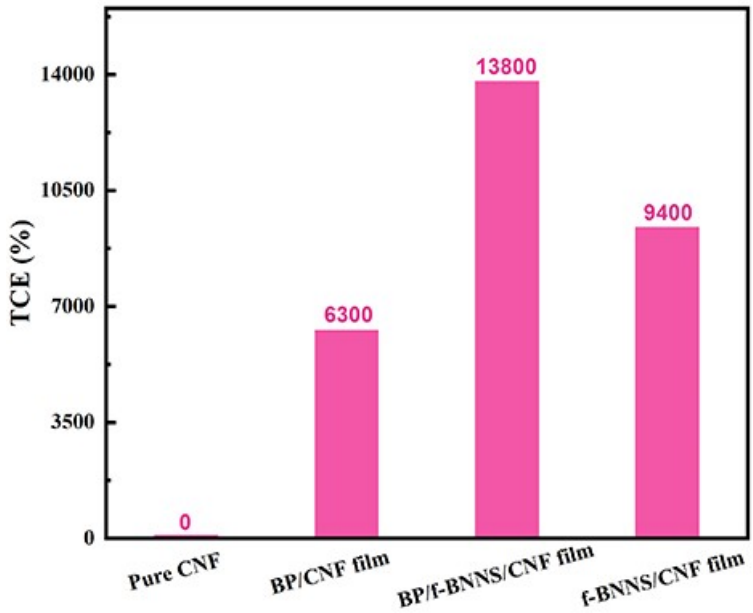

Figure S9. Thermal conductivity enhancement trend of the BP/*f*-BNNS/CNF composite films.

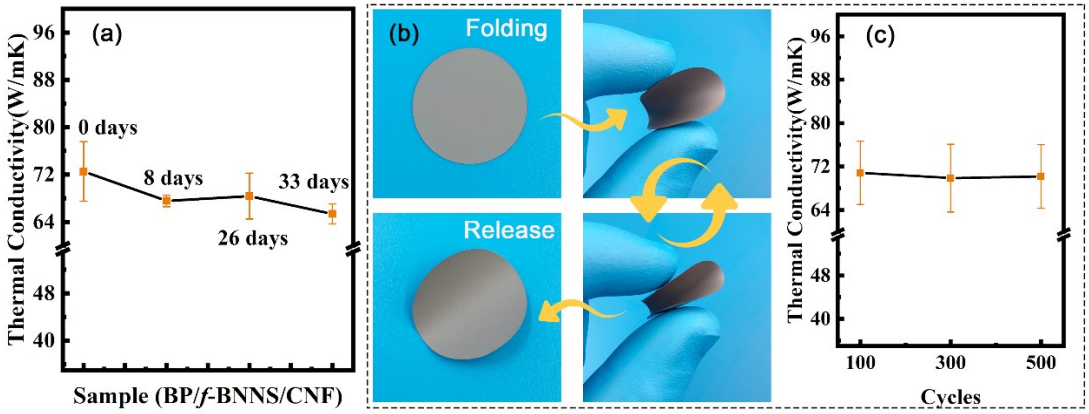

Figure S10. (a)Thermal conductivity one month of BP/*f*-BNNS/CNF composite film; (b) Corresponding morphology of BP/f-BNNS/CNF composite film after bending and (c) in-plane thermal conductivity of this composite film as functions of bending cycles.

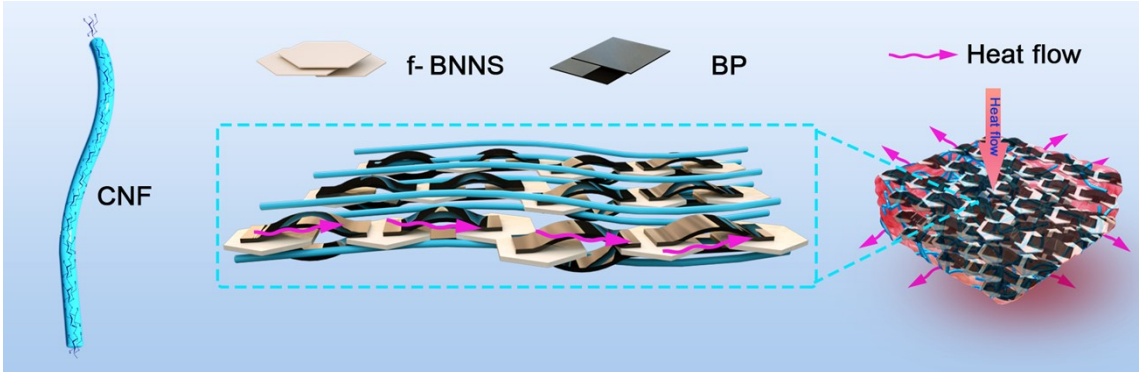

Figure S11. In-plane transfer diagram of heat flow in BP/*f*-BNNS/CNF composite films.

Table S1 Different film surface roughness.

Different films	Sa (μm)		
	Maximum	**Minimum**	**Average**
CNF	2.952	2.952	2.952
BP/CNF	1.360	1.360	1.360
***f*-BNNS/CNF**	1.212	1.212	1.212
BP/*f*-BNNS/CNF	1.19	1.19	1.19